

# Supporting Information

## Interferometric Nanoporous Anodic Alumina Photonic Coatings for Optical Sensing

Yuting Chen<sup>1,2,3</sup>, Abel Santos<sup>1\*</sup>, Ye Wang<sup>1</sup>, Tushar Kumeria<sup>1</sup>, Changhai Wang<sup>2\*</sup>, Junsheng Li<sup>3\*</sup> and  
Dusan Losic<sup>1\*</sup>

<sup>1</sup>School of Chemical Engineering, The University of Adelaide, Engineering North Building, 5005 Adelaide, Australia

<sup>2</sup>Jiangsu Key Laboratory of Marine Biology, College of Resources and Environmental Science, Nanjing Agricultural University, 210095 Nanjing, P. R. China.

<sup>3</sup>College of Food Science and Technology, Nanjing Agricultural University, 210095 Nanjing, P. R. China.

\*E-Mails: [abel.santos@adelaide.edu.au](mailto:abel.santos@adelaide.edu.au) ; [dusan.losic@adelaide.edu.au](mailto:dusan.losic@adelaide.edu.au) ; [chwang@njau.edu.cn](mailto:chwang@njau.edu.cn) ;  
[lijunsheng@njau.edu.cn](mailto:lijunsheng@njau.edu.cn)

## S1. Real-Time Monitoring of $\Delta OT_{eff}$ in RfS

**Figure S1** depicts an example of calculation  $\Delta OT_{eff}$  by applying FFT to the RfS spectrum of a NAA-DBR after infiltration of its nanopores with different solutions and real-time monitoring of effective optical thickness change in a NAA-DBR structure produced with a periodicity of 900 s and 150 anodization pulses. As **Figures S1a and b** show, the RfS spectrum of NAA-DBRs features a maximum of reflection as well as periodically distributed fringes across the spectrum. The application of FFT to the RfS spectrum of NAA-DBRs makes it possible to estimate in an accurate manner the effective optical thickness of the film. Furthermore, as **Figure S1c** depicts,  $\Delta OT_{eff}$  experiences sharp changes after the nanopores of the NAA-DBR photonic coating were filled with liquids of different refractive index ( $n_{water} = 1.333$  RIU,  $n_{glucose\ 0.5M} = 1.349$  RIU,  $n_{ethanol} = 1.362$  RIU and  $n_{isopropanol} = 1.378$  RIU). Note that the total effective optical thickness change was calculated as the difference between the corresponding effective optical thickness and the effective optical thickness of the film when infiltrated with water.

$$\Delta OT_{eff}(Glucose\ 0.5M) = OT_{eff}(Glucose\ 0.5M) - OT_{eff}(Water)$$

$$\Delta OT_{eff}(Ethanol) = OT_{eff}(Ethanol) - OT_{eff}(Water)$$

$$\Delta OT_{eff}(Isopropanol) = OT_{eff}(Isopropanol) - OT_{eff}(Water)$$

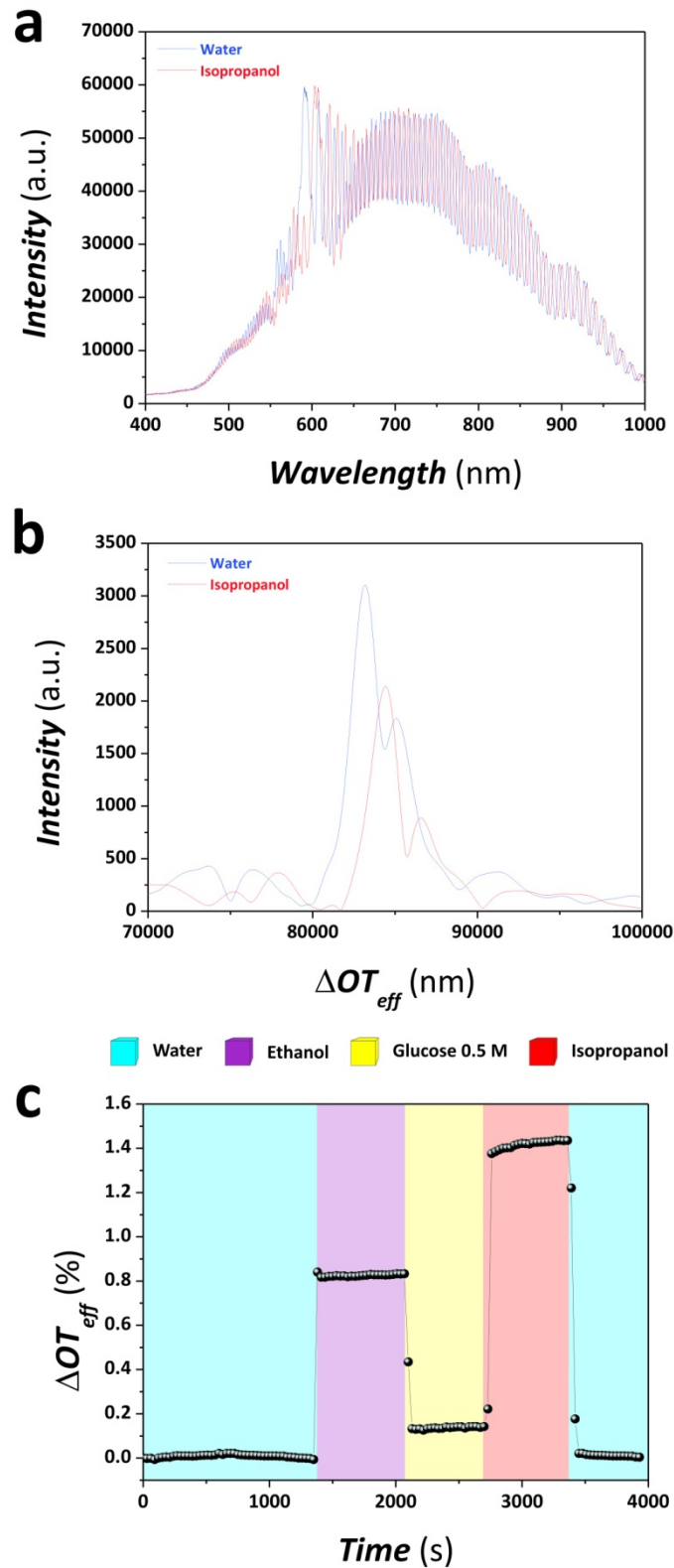


**Figure S1.** Example of real-time monitoring of effective optical thickness change in a NAA-DBR photonic coating (i.e. NAA-DBR<sub>900-150</sub>) after infiltration with ethanol, glucose 0.5 M and isopropanol, respectively.

## S2. Demonstration of Colorimetric Sensing Properties of NAA-DBRs

According to the Fabry–Pérot relationship, the effective optical thickness of NAA-DBR photonic coatings experiences a shift toward longer wavelengths if their nanopores are infiltrated by liquids or gases of higher refractive index than air. NAA-DBR photonic coatings present a highly nanoporous structure (**Figures S2a and b**), which makes it possible to achieve high contrasts of effective refractive index when their nanopores are infiltrated by liquids. **Figure S2c** demonstrates that these photonic coatings experience a sharp red shift in color when their nanopores are filled with a medium with higher refractive index than air (e.g. air –  $n_{air} = 1$  RIU and isopropanol –  $n_{isopropanol} = 1.378$  RIU).

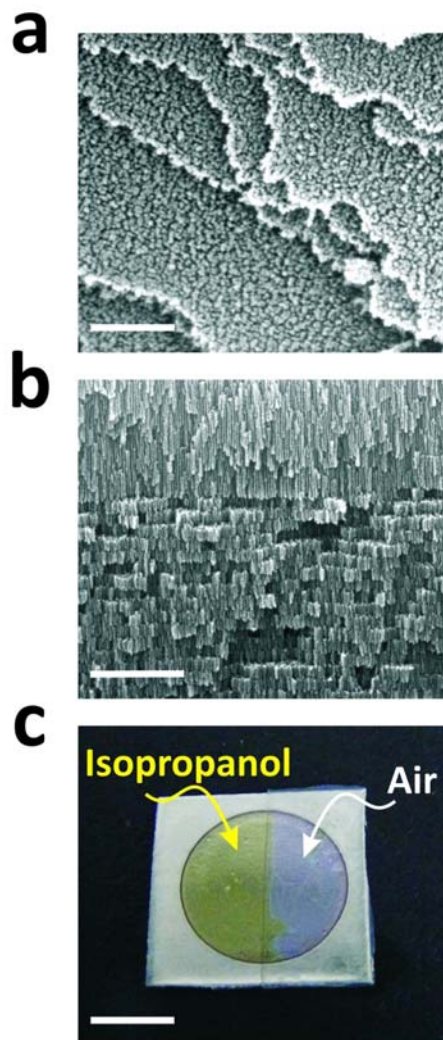


**Figure S2.** Demonstration of colorimetric sensing in NAA-DBRs. a-b) Top and cross-section view SEM images of a NAA-DBR photonic coating (scale bars = 500 nm and 1  $\mu$ m, respectively). c) Digital image of a NAA-DBR (NAA-DBR<sub>675-150</sub>) showing a partial change in color after infiltrating its nanopores with isopropanol (scale bar = 0.5 cm). Note that half NAA-DBR coating was covered with transparent tape in order to avoid the infiltration of its nanopores with isopropanol.

### S3. Linearity of NAA-DBRs

Figure S3 and Table S1 summarize the obtained results of linearity for the different NAA-DBRs analyzed in this study.

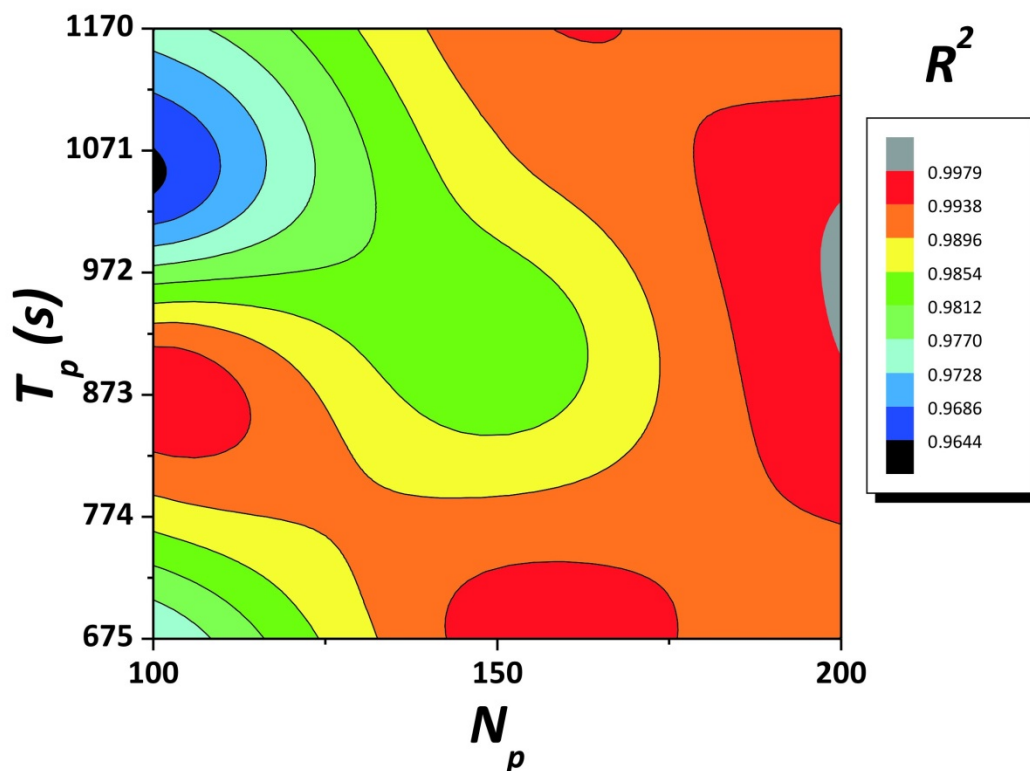


**Figure S3.** Contour plot showing the distribution of the linearity of NAA-DBR photonic coatings obtained from Figure 5 in the manuscript.

**Table S1.** Optical linearity of NAA-DBR photonic coatings assessed by RIFS after infiltration with glucose, ethanol and isopropanol.

NAA-DBR	$R^2$
NAA-DBR <sub>(675-100)</sub>	0.9729
NAA-DBR <sub>(900-100)</sub>	0.9957
NAA-DBR <sub>(1035-100)</sub>	0.9645
NAA-DBR <sub>(1170-100)</sub>	0.9749
NAA-DBR <sub>(675-150)</sub>	0.9959
NAA-DBR <sub>(900-150)</sub>	0.9814
NAA-DBR <sub>(1035-150)</sub>	0.9876
NAA-DBR <sub>(1170-150)</sub>	0.9929
NAA-DBR <sub>(675-200)</sub>	0.9909
NAA-DBR <sub>(900-200)</sub>	0.9978
NAA-DBR <sub>(1035-200)</sub>	0.9978
NAA-DBR <sub>(1170-200)</sub>	0.9913